Organic Electronics 15 (2014) 3756–3760

Contents lists available at ScienceDirect

Organic Electronics

journal homepage: www.elsevier.com/locate/orgel

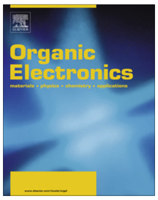

Highly efficient organic tandem solar cell based on SubPc:C_{70} bulk heterojunction

Fangming Jin [a,b], Bei Chu [a], Wenlian Li [a,*], Zisheng Su [a,*], Xingwu Yan [a,b], Junbo Wang [a], Ruigang Li [a], Bo Zhao [a,b], Tianyou Zhang [a,b], Yuan Gao [a,b], C.S. Lee [c], Hairuo Wu [a,b], Fuhua Hou [a,b], Tong Lin [a,b], Qiaogang Song [a,b]

[a] *State Key Laboratory of Luminescence and Applications, Changchun Institute of Optics, Fine Mechanics, and Physics, Chinese Academy of Sciences, Changchun 130033, People's Republic of China*
[b] *University of Chinese Academy of Sciences, Beijing 100039, People's Republic of China*
[c] *Center of Super-Diamond and Advanced Films (COSDAF), City University of Hong Kong, Hong Kong*

ARTICLE INFO

Article history:
Received 25 August 2014
Received in revised form 11 October 2014
Accepted 13 October 2014
Available online 31 October 2014

Keywords:
Tandem OSC
Bulk heterojunction
Low-concentration donor
F16CuPc

ABSTRACT

Highly efficient organic tandem solar cell with peak power conversion efficiency (PCE) of 7.66% has been demonstrated by simply stacking two same boron subphthalocyanine (SubPc):C_{70} bulk heterojunction devices, with a high active inter-connecting layer composed of bathophenanthroline (Bphen)/Silver/hexadecafluoro-copper-phthalocyanine (F_{16}CuPc)/MoO_3. We find that F_{16}CuPc plays an important role which extends the recombination zone, facilitates the extraction of hole and the carrier recombination. The measured PCE of the tandem solar cell corresponds to a 38% increase compared to that the optimal single cell.

1. Introduction

Organic solar cells (OSCs) have attracted much attention as a promising renewable energy source because of the potential for low cost production of energy, simple fabrication process and high flexibility. Further improvement of PCE is still required for commercialization, although maximal power conversion efficiency (PCE) of OSCs have reached to 10% through a combination of synthesis of novel materials and device engineering [1]. Essential properties of the organic semiconductors which are narrow absorption bandwidth, short exciton diffusion length and low charge carrier mobility, however, limit OSCs' performance improvement. Thus, maximizing light absorption by increasing the thickness of the layers can reduce the carrier collection efficiency and make the cell too resistive, which will have an impact on its performance. In order to overcome these obstacles, tandem cell in series is developed, which is considered to be an effective way to get an efficiency above 15% [2]. For a tandem solar cell, two or more OSCs are connected in series by stacking them on top of one another, with an interlayer connecting two adjacent cells, referred to as inter-connecting layer (ICL). The ICL plays a very critical role for the tandem OSC performance since it needs to facilitate efficient recombination of opposite charge carriers coming from the adjacent OSCs. Excellent ICL should possesses following properties: (1) low electrical resistance, (2) high optical transparency, (3) low barriers for both electron and hole extraction, (4) simple-fabrication process. Efficient ICL for carrier recombination between subcells has been shown in literatures using thin metal layers [3], highly doped organic layers [4], or metal-oxides [5]. Typically, two or more subcells with complementary absorption spectra are used in a series-connected tandem cell to improve the overall

---

[*] Corresponding authors. Tel./fax: +86 0431 86176345.
E-mail addresses: wllioel@aliyun.com (W. Li), suzs@ciomp.ac.cn (Z. Su).

http://dx.doi.org/10.1016/j.orgel.2014.10.019
1566-1199/

absorption and to provide a matched photocurrent from individual subcells [6]. Subcells with identical compositions have also been used in tandem structure, however, what is a pity that, seldom high efficient tandem OSCs with identical compositions were reported [7].

Recently, small molecular bulk heterojunction OSCs with a low donor concentration have gained considerable interest [8,9]. Such fullerene-based (C_{60} or C_{70}) small molecular bulk heterojunction OSCs provide high open-circuit voltage (V_{oc}) of ~1 V due to the presence of n-type Schottky junction formed between fullerene and an adjacent high work function anode of MoO_3. Donor material with low concentrations doped into the fullerene matrix serves as efficient exciton dissociation and hole transport agents that can boost short-circuit currents substantially. As a consequence, fullerene-based OSCs with a low donor concentration have been demonstrated to provide some of the highest-performance vacuum-deposited small molecule OSCs, with PCE up to 8.1% by incorporating a improved combined cathode buffer layer [10]. It is expected that introducing bulk heterojunction OSCs with low donor concentration as the subcells into a tandem cell can substantially increase the efficiency of OSCs, but such reports are still rare to date [11,12].

In this report, the tandem cells were structured by simply stacking two same subphthalocyanine (SubPc):C_{70} bulk heterojunction subcells, with a high active ICL consisted of bathophenanthroline (Bphen)/Silver/hexadecafluoro-copper-phthalocyanine (F_{16}CuPc)/MoO_3. As a result, we demonstrated a highly efficient organic tandem solar cell with peak PCE of 7.66%. The tandem cell reaches a high V_{oc} of 2.00 V, which almost equals the sum of the V_{oc} of the individual cells. Interestingly, a better FF from 0.45 to 0.52 compared to the single cell was observed. Finally, the efficiency of the stacked device increases by 38% compared with the optimized single cell.

2. Experiment methods

Materials for fabrication were procured commercially and were used without further sublimation. Organics and metal layers were sequentially deposited onto the clean patterned ITO glass substrates with a sheet resistance of 20 Ω/sq via shadow masks to form devices with an area of 0.1 cm^2. Prior to deposition, the ITO surface was cleaned in a series of solvents and then treated by ultraviolet–ozone in a chamber for 15 min. Deposition rates were monitored with a quartz oscillating crystal and controlled to be 0.05 nm/s for organic layer and 0.5 nm/s for metal layers. Absorption and transmittance spectra of the organic films and ICL on ITO substrates were measured with a Shimadzu UV-3101 PC spectrophotometer with ITO substrates as the reference samples in the experiments. Current density–voltage (J–V) characteristics are measured in the dark and under simulated solar illumination, using a Keithley 2400 measurement unit. For the incident photon-to-current conversion efficiency (IPCE) measurements, light from Xe lamps is coupled into a monochromator and their intensities are calibrated with a Si-photodiode. The light incident on the device is chopped and the modulated current signal is detected with a current–voltage and lock-in amplifier. All the measurements were carried out at room temperature under ambient conditions.

3. Results and discussion

Before the fabrication of tandem OSCs, we firstly investigated the photovoltaic performance of the single cells, with a structure of ITO/MoO_3 (10 nm)/SubPc:C_{70} (10%, 50 nm)/Bphen (6 nm)/Al (100 nm). The weight ratio of SubPc:C_{70} films was optimized to be 1:10 and was fixed in the next work. The doping concentration is higher than that reported in the Refs. [8,9], which may be resulted from the appearance of nanocrystalline domains of SubPc in mixed films containing 10% SubPc [13] and from extra photocurrent contributed by the strong light absorption of SubPc. The absorption spectra of SubPc and C_{70} films are shown in Fig. 1(a). SubPc is composed of three N-fused diiminoisoindole rings centered around a boron core (Fig. 1(b)). Such nonplanar structure influences the molecular packing and hence film morphology under different deposition conditions [14]. SubPc shows an absorption range between 500 and 610 nm and C_{70} between 300 and 700 nm, which are complementary and give a wide spectral coverage. Fig. 1(b) depicts the current density–voltage (J–V) characteristics of optimized single cell under simulated AM 1.5 G illumination at 100 mW/cm^2. A peak PCE of 5.55% with J_{SC} = 12.04 mA/cm^2, V_{oc} = 1.03 V, and FF = 0.45 is realized in uniformly mixed OSCs containing 10 wt.% SubPc. Such performance is comparable to a previous report [15].

Fig. 2(a) plots the IPCE measurements of the single cell and the normalized absorption spectra for 50-nm-thick SubPc:C_{70} film with blend ratio of 1:10. There is a disparity between IPCE and absorption spectra at $\lambda < 390$ nm which is resulted from the low transmittance of ITO and the parasitic absorption in the buffer layers of Bphen and MoO_3. The response occurring at wavelengths $\lambda < 500$ nm originates mainly from C_{70} while the response at longer wavelengths corresponds to absorption in both SubPc and C_{70}. As shown in Fig. 2(a), the IPCE spectra consist of three major peaks at 390 nm, 520 nm and 580 nm approximately. The first two peaks located at 390 nm and 520 nm respectively, correspond to absorption of C_{70}, and the third peak at 580 nm is from SubPc. The average IPCE in visible range is between 50% and 60%, indicating that nearly a half of photons is wasted and does not contribute to the photocurrent, which provides a large space to increase the performance of the tandem device with subcells have the same compositions.

The structure of the tandem OSCs used here is ITO/MoO_3 (5 nm)/ SubPc:C_{70} (T1 nm)/Bphen (2 nm)/Ag (0.5 nm)/F_{16}CuPc (1 nm)/MoO_3 (5 nm)/SubPc:C_{70} (T2 nm)/Bphen (6 nm)/Al (100 nm) as shown in Fig. 2(b). Here, the subcells are connected using an optimized recombination zone, consisting of 2 nm Bphen, nominal 0.5 nm Ag, 1 nm F_{16}CuPc and 5 nm MoO_3. The transmittance spectrum of the ICL Bphen (2 nm)/Ag (0.5 nm)/F_{16}CuPc (1 nm)/MoO_3 (5 nm) is shown in Fig. 1. It can be seen that the transmittance is almost 95% in the range from 400 to 800 nm, ensuring enough light to be absorbed by the top cell. Hence, this ICL with high transparency satisfies the optical requirement as outlined in the beginning. Two subcells are both composed of SubPc:C_{70} (10%). A series of tandem cells

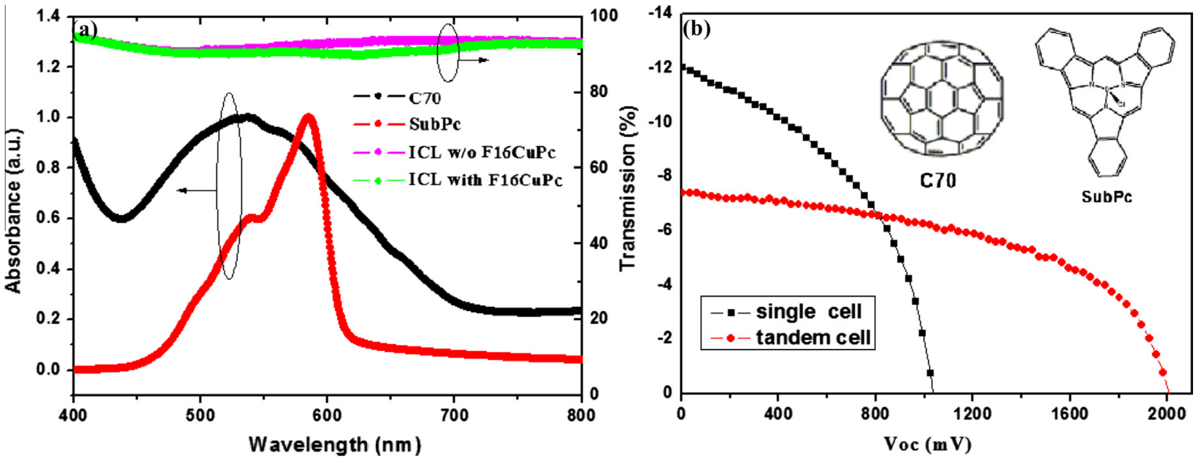

Fig. 1. (a) Absorption spectra of neat C_{60} and SubPc films and the transmittance spectrum of the ICL Bphen (2 nm)/Ag (0.5 nm)/$F_{16}CuPc$ (1 nm)/MoO_3 (5 nm) on ITO substrate. (b) *J–V* characteristics under 1 sun, AM 1.5G illumination for the optimized single and tandem cells. The inset is the molecular structure of SubPc and C_{70}.

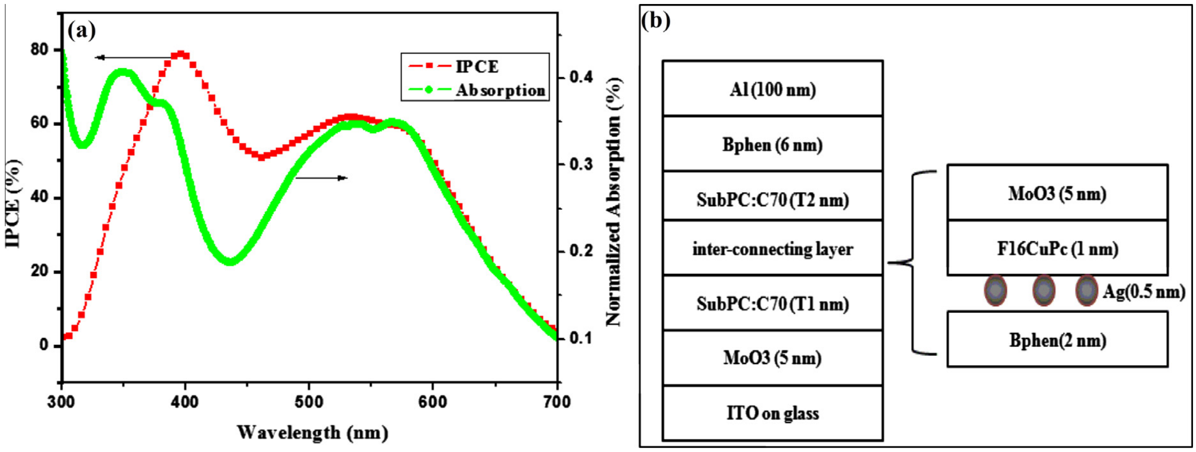

Fig. 2. (a) IPCE of the single cell ITO/MoO_3 (5 nm)/SubPc:C_{70} (10%, 50 nm)/Bphen (6 nm)/Al (100 nm) and normalized absorption spectrum of SubPc:C_{70} (10%, 50 nm). (b) Schematic of the tandem OSC structure.

with different thickness of T1 and T2 were fabricated in older to optimize performance of the tandem cell.

Table 1 summarizes the extracted parameters for the devices. The experimentally measured V_{oc} of the tandem cells nearly equals the double of the single cell as expected reaching to as high as about 2 V, demonstrating the correct operation of the series connected tandem architecture and the effectiveness of the interlayer. The small variation of the V_{oc} is easily understood by considering that the V_{oc} of subcell itself is increased with the active layer thickness for such low donor concentration based bulk heterojunction cell [16]. Subcell thickness affects markedly on the tandem cell performance. Compare with the bottom cell, such influence becomes more pronounced for the top cell. For example, J_{SC} varies between 4.00 mA/cm^2 and 4.46 mA/cm^2 (in ca. 12%), 6.50 mA/cm^2 and 7.38 mA/cm^2 (in ca. 13%), 6.04 mA/cm^2 and 6.90 mA/cm^2 (in ca. 14%) at thickness of bottom cell changes from 30 nm to 50 nm when thickness of top cell is fixed as 30, 40 and 50 nm, respectively. While the thickness of bottom cell is fixed at 30, 40 and 50 nm, J_{SC} varies in a larger range, i.e., from 4.46 mA/cm^2 to 7.38 mA/cm^2 (in ca. 65%), 4.13 mA/cm^2 to 6.90 mA/cm^2 (in ca. 67%), 4.00 mA/cm^2 to 6.78 mA/cm^2

Table 1
Performance summery of tandem OSCs with different thickness of bottom and top subcells.

Devices (T1, T2, nm)	J_{SC} (mA/cm^2)	V_{oc} (V)	FF	PCE (%)
Single cell	12.04	1.03	0.45	5.55
(30, 30)	4.46	1.98	0.53	4.68
(30, 40)	7.38	2.00	0.52	7.66
(30, 50)	6.04	2.00	0.48	5.80
(40, 30)	4.13	1.99	0.51	4.19
(40, 40)	6.57	2.02	0.49	6.50
(40, 50)	6.90	1.99	0.45	6.17
(50, 30)	4.00	2.02	0.50	4.04
(50, 40)	6.50	1.97	0.47	6.01
(50, 50)	6.78	1.98	0.43	5.78

(in ca. 70%) as thickness of top cell changes from 30 nm to 50 nm. Thus, device performance is mainly restricted by the top cell. It is known that matched J_{SC} of bottom and top single cells is critically important for achieving high photovoltaic response of the tandem cells in series. In our case, since bottom and top single cell are constructed with the same composition, a thicker top cell is needed to extract more light and to produce a same photocurrent with the bottom cell. Indeed, relative high J_{SC} and PCE were all obtained by the devices that the top cell is thicker than that of the bottom cell.

The thickness of bottom cell and top cell for the most efficient tandem cell is 30 nm and 40 nm, respectively. The *J–V* characteristics of the most efficient tandem and reference single cells taken under AM1.5G 100 mW/cm^2 illumination are shown in Fig. 1(b) and photovoltaic parameters are listed in Table 1. The best tandem cell yields a PCE of 7.66% with a J_{SC} of 7.38 mA/cm^2, a V_{oc} of 2.00 V and a FF of 0.52. The J_{SC} in the tandem cell remains 61% compared to the J_{SC} in the most efficient single-cell device, indicating that more photos are utilized for the photocurrent generation. With FF increase from 0.44 to 0.52 combined with a doubled V_{oc}, as a result, PCE of the tandem cell increases by 38% compared with the optimized single cell.

Fig. 3 plots FF as a function of sum thickness of bottom and top cell. One can see that FF manifests an approximate linear decrease with the sum thickness increases. For the cells with the same total thickness, the thinner bottom cell based tandem cells show a better FF, implying more balanced photocurrent in the two subcells which is in accordance with previous description. It is remarkable that most tandem cells with different T1 and T2 show a higher FF than that of the single cell. Similar results were reported by other groups [17], and an analytical model was presented recently [18]. For our devices here, a higher FF may be attributed to several following reasons: (1) light intensity is distributed at two subcells and current density of the tandem cell is much smaller than that of the single cell, which suppress non-germinated recombination of devices. Non-germinated recombination is quite severe in such Schottky junction based bulk heterojunction OSCs, and a linear decrease of FF with increase incident light power density was observed by Chen etc. [19]. Suppressing non-germinated recombination by a decreased photocurrent pushes a higher FF. (2) The ICL of the tandem cell may function more efficiently than the electrode buffer layer in a single cell, which is assumed to be attributed to the effect of F_{16}CuPc. In order to confirm this assumption, devices without F_{16}CuPc in ICL were constructed. Fig. 4 depicts the *J–V* characteristics of the tandem cells (T1 = 30 nm, T2 = 40 nm; T1 = 50 nm, T2 = 50 nm) with or without 1 nm F_{16}CuPc in ICL under 100 mW/cm^2 AM 1.5G illumination and their parameters are summarized in Table 2. Compared with the traditional ICL with the structure of Bphen/Ag (or Al)/MoO$_3$ used in small molecular tandem OSCs, inserting 1 nm F_{16}CuPc between Ag and MoO$_3$ improves devices performance greatly. It can be seen that the inclusion of 1 nm F_{16}CuPc results in FF increases remarkably from 0.37 and 0.44 to 0.43 and 0.52, respectively, and the J_{SC} also increases a little simultaneously. Recently, our group demonstrated an improved performance of the OSCs by using an electron transport material F_{16}CuPc as an anode buffer layer [20]. More recently, we also reported that inserting an organic heterointerface layer composed of F_{16}CuPc/1,1-bis-(4-methyl-phenyl)-aminophenylcyclohexane (TAPC) can great improve the performance of OSCs [21]. The improvement with introducing F_{16}CuPc or organic heterointerface composed of F_{16}CuPc is achieved by promoting extraction of holes, in which holes collection with F_{16}CuPc relies on the recombination at the interface of donor (or anode buffer layer)/F_{16}CuPc with electrons injected from ITO anode via the LUMO of F_{16}CuPc and holes injected from donor or anode buffer layer. It can be seen from the schematic diagram of the ICL interfacial energetic (Fig. 5) that without F_{16}CuPc charge recombination only occurs at Ag nanoparticles which are sparsely distributed [22] and may behave less than effective. When 1 nm F_{16}CuPc inserted, electrons in the bottom cell can transport via the LUMO of F_{16}CuPc reaching to the interface of F_{16}CuPc/MoO$_3$ and recombine at the interface with holes

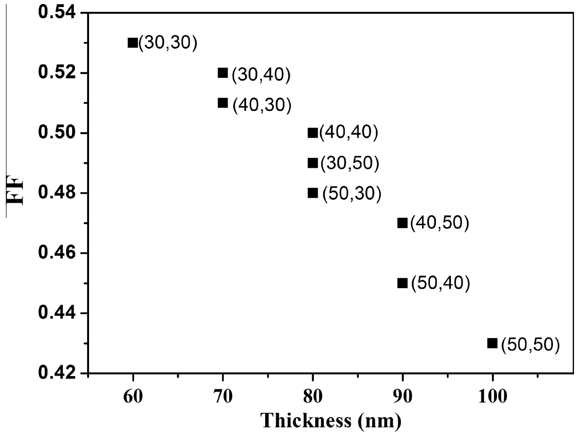

Fig. 3. FF as a function of total thickness of bottom and top cells.

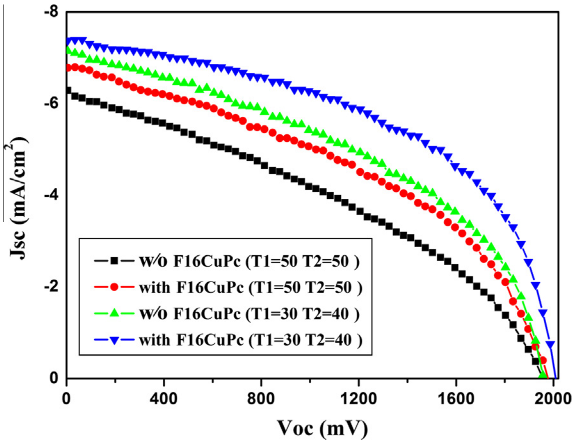

Fig. 4. *J–V* characteristics of the tandem cells (T1 = 30 nm, T2 = 40 nm; T1 = 50 nm, T2 = 50 nm) with or without 1 nm F_{16}CuPc in inter-connecting layer under 100 mW/cm^2 AM 1.5G illumination.

Table 2
Comparison of the performance of the OSCs with or without 1 nm $F_{16}CuPc$ in the inter-connecting layer.

Devices (T1, T2, nm)	J_{SC} (mA/cm^2)	V_{oc} (V)	FF	PCE (%)
(30, 40) (w/o F16CuPc)	7.14	1.96	0.45	6.30
(30, 40) (with F16CuPc)	7.38	2.00	0.52	7.66
(50, 50) (w/o F16CuPc)	6.29	1.96	0.38	4.67
(50, 50) (with F16CuPc)	6.78	1.98	0.43	5.78

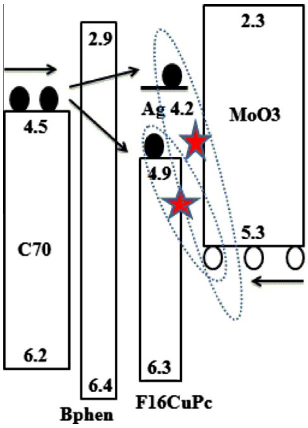

Fig. 5. The schematic energy level diagram of the ICL Bphen (2 nm)/Ag (0.5 nm)/$F_{16}CuPc$ (1 nm)/MoO_3 (5 nm). Electrons and holes are shown as filled and open circles, respectively. The energy levels are given in units of eV.

generated in the top cell come. Hence, in the case of the tandem cell here, $F_{16}CuPc$ is believed to extend the recombination zone and to facilitate the extraction of hole and the recombination of the electron and hole, which make the ICL work more actively and boost the performance of the tandem cell. In a word, inclusion of $F_{16}CuPc$ does improve the photovoltaic response of the tandem cells, and a more detailed working mechanism is under research.

4. Conclusion

Tandem organic solar cell with a PCE of 7.66% was achieved. By simply stacking two same SubPc:C70 bulk heterojunction devices, with a high active improved ICL composed of Bphen/Silver/$F_{16}CuPc$/MoO_3, we obtained a 38% increase in PCE compared to the optimal single cell. Our results demonstrate the superiority of the tandem OSCs based on low donor concentration bulk heterojunction. What is more, we find that highly efficient tandem OSCs consisted of the subcells with same active materials can be constructed by using an active ICL.

Acknowledgments

This work was supported by the National Natural Science Foundation of China (61376062, 61376022, 61107082, and 11004187), and the Science and Technology Development Plan of Jilin Province (20140101094JC).

References

[1] J. You, L. Dou, K. Yoshimura, T. Kato, K. Ohya, T. Moriarty, K. Emery, C. Chen, J. Gao, G. Li, Y. Yang, A polymer tandem solar cell with 10.6% power conversion efficiency, Nat. Commun. 4 (2013) 1446.

[2] G. Dennler, M.C. Scharber, T. Ameri, P. Denk, K. Forberich, C. Waldauf, C.J. Brabec, Design rules for donors in bulk-heterojunction tandem solar cells-towards 15% energy-conversion efficiency, Adv. Funct. Mater. 20 (2008) 579–583.

[3] D. Zhao, X. Sun, C. Jiang, A.K. Kyaw, G.Q. Lo, D.L. Kwong, Efficient tandem organic solar cells with an Al/MoO_3 intermediate layer, Appl. Phys. Lett. 93 (2008) 083305.

[4] R. Timmreck, S. Olthof, K. Leo, M.K. Riede, Highly doped layers as efficient electron–hole recombination contacts for tandem organic solar cells, J. Appl. Phys. 108 (2010) 033108.

[5] D.J.D. Moet, P. de Bruyn, P.W.M. Blom, High work function transparent middle electrode for organic tandem solar cells, Appl. Phys. Lett. 96 (2010) 153504.

[6] K. Li, Z. Li, K. Feng, X. Xu, L. Wang, Q. Peng, Development of large band-gap conjugated copolymers for efficient regular single and tandem organic solar cells, J. Am. Chem. Soc. 135 (2013) 13549–13557.

[7] K. Kawano, N. Ito, T. Nishimori, J. Sakai, Open circuit voltage of stacked bulk heterojunction organic solar cells, Appl. Phys. Lett. 88 (2006) 073514.

[8] M. Zhang, H. Wang, H. Tian, Y. Geng, C.W. Tang, Bulk heterojunction photovoltaic cells with low donor concentration, Adv. Mater. 23 (2011) 4960–4964.

[9] F. Jin, B. Chu, W. Li, Z. Su, B. Zhao, T. Zhang, X. Yan, Y. Gao, H. Wu, C.S. Lee, J. Zhu, H. Pi, J. Wang, The influence of donor material on achieving high photovoltaic response for organic bulk heterojunction cells with small ratio donor component, Org. Electron. 14 (2013) 1130–1135.

[10] X. Xiao, K.J. Bergemann, J.D. Zimmerman, K. Lee, S.R. Forrest, Small-molecule planar-mixed heterojunction photovoltaic cells with fullerene-based electron filtering buffers, Adv. Energy Mater. 4 (2014) 1301557.

[11] M. Zhang, H. Wang, C.W. Tang, Tandem photovoltaic cells based on low-concentration donor doped C60, Org. Electron. 13 (2012) 249–251.

[12] D. Cheyns, M. Kim, B. Verreet, B.P. Rand, Accurate spectral response measurements of a complementary absorbing organic tandem cell with fill factor exceeding the subcells, Appl. Phys. Lett. 104 (2014) 093302.

[13] R. Pandey, A.A. Gunawan, K.A. Mkhoyan, R.J. Holmes, Efficient organic photovoltaic cells based on nanocrystalline mixtures of boron subphthalocyanine chloride and C60, Adv. Funct. Mater. 22 (2012) 617–624.

[14] K. Vasseur, K. Broch, A.L. Ayzner, B.P. Rand, D. Cheyns, C. Frank, F. Schreiber, Michael F. Toney, L. Froyen, P. Heremans, Controlling the texture and crystallinity of evaporated lead phthalocyanine thin films for near-infrared sensitive solar cells, Appl. Mater. Interface 5 (2013) 8505–8515.

[15] R. Pandey, Y. Zou, R.J. Holmes, Efficient bulk heterojunction organic photovoltaic cells based on boron subphthalocyanine chloride-C70, Appl. Phys. Lett. 101 (2012) 033308.

[16] Y. Zheng, W.J. Potscavage Jr., T. Komino, M. Hirade, J. Adachi, C. Adachi, Highly efficient bulk heterojunction photovoltaic cells based on C70 and tetraphenyldibenzoperiflanthene, Appl. Phys. Lett. 102 (2013) 143304.

[17] J. Yang, W. Chen, B. Yu, H. Wang, D. Yan, Organic tandem solar cell using active inter-connecting layer, Org. Electron. 13 (2012) 1018–1022.

[18] B.E. Lassiter, C.K. Renshaw, S.R. Forrest, Understanding tandem organic photovoltaic cell performance, J. Appl. Phys. 113 (2013) 214505.

[19] G. Chen, H. Sasabe, Z. Wang, X. Wang, Z. Hong, Y. Yang, J. Kido, Co-evaporated bulk heterojunction solar cells with > 6.0% efficiency, Adv. Energy Mater. 24 (2012) 2768–2773.

[20] Y. Liu, B. Chu, Z. Su, W. Li, T. Zhang, F. Jin, X. Yan, B. Zhao, F. Zhang, Di Fan, J. Wang, Y. Gao, Mechanisms of the improved organic photovoltaic performance by using electron-transporting CuPc derivative as anode modifying layer, Org. Electron. 13 (2012) 2865–2869.

[21] X. Yan, B. Chu, W. Li, Z. Su, T. Zhang, F. Jin, B. Zhao, F. Zhang, Di Fan, Y. Gao, T. Tsuboi, J. Wang, H. Pie, J. Zhu, Improved photovoltaic characteristics of organic cells with heterointerface layer as a hole-extraction layer inserted between ITO anode and donor layer, Org. Electron. 14 (2013) 1805–1810.

[22] Z. Su, L. Wang, Y. Li, G. Zhang, H. Zhao, H. Yang, Y. Ma, Bei Chu, W. Li, Surface plasmon enhanced organic solar cells with a MoO_3 buffer layer, Appl. Mater. Interface 5 (2013) 12847–12853.